Conference Paper, Published Version

Orimoloye, Stephen; Horrillo-Caraballo, Jose; Karunarathna, Harshinie; Reeve, Dominic

Modelling Wave Overtopping of Steep Impermeable Structures under Bimodal Sea Conditions

Coastal Structures 2019 - Nils Goseberg, Torsten Schlurmann (eds) - © 2019 Bundesanstalt für Wasserbau
ISBN 978-3-939230-64-9 (Online) - DOI: 10.18451/978-3-939230-64-9_121

Modelling Wave Overtopping of Steep Impermeable Structures under Bimodal Sea Conditions

A. S. Orimoloye, J. Horrillo-Caraballo, H. Karunarathna & D. E. Reeve
Energy and Environment Research Group, Zienkiewicz Centre for Computational Engineering, College of Engineering, Swansea, SA1 8EN, United Kingdom.

Abstract: Prediction of wave overtopping is a crucial component of coastal structure and seawall designs. Modelling efforts have improved coastal seawall construction design and have saved construction costs. Despite a large amount of research on wave overtopping as published in the EurOtop (2018), there are still knowledge gaps to be considered in terms of swell and bimodal sea states. Specifically, how the distribution of wave energy across swell and wind wave components affects the overtopping rates. Generally, bimodal sea conditions containing swell have been constructed from the superposition of two JONSWAP spectra; one representing the wind sea and one the swell. In the present study, we investigate the average wave overtopping of an impermeable sea seawall under unimodal and bimodal wave conditions in 2D physical model tests. Overtopping rates increase with increasing swell percentages but show few variations when compared with the position of the swell peaks in the bimodal spectrum. Shallow water effects appear to be more significant for steeper slopes than milder ones but are not enough to create any noticeable trends in the relative wave overtopping estimates in the deep-water conditions studied here. The most recent EurOtop formula accurately predict the relative overtopping rates for the unimodal cases but underestimate the measured overtopping in the bimodal conditions investigated.

Keywords: unimodal waves, swells, bimodal spectrum, energy-conserved, wave overtopping

1 Introduction

Prediction of wave overtopping is a crucial component of coastal structure and seawall designs. During the design of coastal seawalls, sea states described by the integrated spectral parameters H_{m0} and $T_{m-1,0}$ are usually taken as crucial input variables. However, sea states are complicated and are predominantly created by the influence of the wind (from the local wind sources) and grow systematically until they decay. The decay processes are gradual and are usually accompanied by the transfer of energy from higher to lower frequencies (in the form of swell). As described in Hawkes et al., (1998), and Reeve et al., (2015), combinations of swell and wind waves often result in more irregular randomness of the sea. Wind waves possess simple configuration and are easier to predict because they are characterized by one spectral peak (unimodal spectrum) with one significant wave height and one spectral peak period, (Biesel, 1951; Burcharth, 1978; Battjes and Groenendijk, 2000; Krogstad and Arntsen, 2000). A double-peaked bimodal spectrum occurs when local wind waves are combined with swell.

Analyses of the characteristics of bimodal waves have shown a significant complexity from what is expected when separate analysis of the individual swell or the wind waves are carried out (Rychlik et al., 1997; Brodtkorb et al., 2000). According to Hawkes et al. (1998), bimodal waves may be the worst-case sea conditions that a sea defence or beaches could experience because the combined effects of swell and wind waves could produce extreme results.

Physical modelling techniques have been used extensively to investigate wave-structure interactions and wave overtopping of coastal structures under unimodal sea conditions, (e.g. Goda et al., 1975; Owen, 1982; and Franco et al., 1994). These studies provide guidance and data for wave

overtopping estimates of coastal defences. Further, De Rouck et al. (2009) provide a summary of numerous wave overtopping datasets compiled on different physical experiments covering various seawall geometries. More details of these studies can be found in Troch et al. (2004); De Rouck et al. (2005); Franco et al. (2009). These databases have been valuable and have been presented by van der Meer et al. (2005 & 2009) or more comprehensively in Pullen et al. (2007). Recently, a series of wave overtopping tests have been performed at Ghent University (Belgium). These are presented in Gallach-Sánchez et al. (2011) and also in Victor and Troch (2012) focusing primarily on steep low-crested coastal seawalls in deep and shallow water conditions. Based on these studies and many more, some significant modified wave overtopping formulations have been made (Van der Meer and Bruce, 2014; Van der Meer et al., 2018). Concerning wave overtopping estimates for bimodal seas, Hawkes et al., (1998) have presented physical model tests, and Thompson et al. (2017) showed a numerical assessment of overtopping performance of a simple coastal seawall under bimodal seas. The influence of wave directionality on wave overtopping oblique wind and swell waves was recently investigated by Van der Werf and Van Gent (2018).

The present study aims to better understand wave overtopping characteristics of coastal seawalls under attack from bimodal sea conditions. Commonly, bimodal sea conditions containing swell have been constructed from the superposition of two JONSWAP spectra; one is representing the wind sea and one the swell. With this construction, there will be a degree of overlap between the spectra and a sharp break between the swell and the wind sea as a separation frequency is not present. This contrasts with the practice-based approach in which the swell and wind-sea components have no overlap (Bradbury et al., 2007). Here, we use the former method to create a set of bimodal sea states that have varying proportions of swell, while at the same time containing a fixed amount of energy. We refer to a set of sea states that have a fixed amount of energy but varying proportions of swell and wind sea as 'energy conserved' bimodal waves. The extremes of these conditions are 'pure wind sea' at one end and 'pure swell' at the other; with both cases resulting in a unimodal spectrum. The details of generating such sea states have been described in Orimoloye et al. (2019). In the present study, we investigate the average wave overtopping of an impermeable sea seawall under bimodal wave conditions. Specifically, we are interested in whether changes in the distribution of wave energy across swell and wind wave components have a quantifiable effect on the overtopping rates. The paper is divided into five sections; Section 2 focuses on previously published wave overtopping prediction formulations. Section 3 describes the experimental tests; results and discussions are presented in section 4, while Section 5 concludes the paper.

2 Prediction of relative wave overtopping

Owen (1982) proposed a decreasing exponential relationship between the wave overtopping q by a coastal seawall with respect to the crest freeboard R_c. This can be expressed mathematically as:

$$\frac{q}{\sqrt{gH_{m_0}^3}} = \mathrm{a}.\exp\left(-\mathrm{b}\,\frac{\mathrm{R_c}}{\mathrm{H_{mo}}}\right) \tag{1}$$

In Eq. (1), H_{m0} represents the spectral significant wave height at the toe of the structure, a and b are the fitted coefficients. Note that coefficients a and b presented in Eq. (1) have been given several definitions over the years. Further, the entire relationship between dimensionless wave overtopping $q/\sqrt{(H_{m0}{}^3)}$ and the relative crest freeboard has been refined by different authors. These refinements are in the context of accommodating several other influence factors due to berms γ_b, permeability and roughness γ_f, for oblique wave attack, γ_β, influence factor by a vertical wall γ_v and different geometries γ^*. Also, g represents the acceleration due to gravity and $\xi_{m-1,0}$ is the surf similarity parameter or the Iribarren number. New sets of wave overtopping formulae, as summarized in EurOtop (2018) are presented in Eq. (2) for the mean wave overtopping rate under breaking wave conditions and Eq. (3) for the overtopping rate under non-breaking wave conditions:

$$\frac{q}{\sqrt{gH_{mo}^3}} = 0.023 \times \gamma_b \times \xi_{m-1,0} \times \exp\left[-\left(2.7 \frac{R_c}{\xi_{m-1,0} H_{m0} \times \gamma_b \times \gamma_f \times \gamma_\beta \times \gamma_v}\right)^{1.3}\right] \quad (2)$$

$$\frac{q}{\sqrt{gH_{mo}^3}} = 0.09 \times e\exp\left[-\left(1.5 \frac{R_c}{H_{m0} \times \gamma_f \times \gamma_\beta \times \gamma^*}\right)^{1.3}\right] \quad (3)$$

Equations (2) and (3) have an exponent of 1.3 instead of 1.0 contained in EurOtop (2007) formulations.

The latest improvement to the Eurotop (2018) formulations is the possibility to generalize appropriate coefficients across different slopes of an impermeable seawall under non-breaking waves conditions as presented in Eq. (4) below. More details can be found in Van der Meer and Bruce, (2014):

$$\frac{q}{\sqrt{gH_{mo}^3}} = a \times e\exp\left[-\left(b \frac{R_c}{Hm_0 \times \gamma_f \times \gamma_\beta}\right)^c\right] \quad (4)$$

Values of coefficients *a* and *b* for can be defined for sloping structures as follows:

$$a = \begin{cases} 0.09 + 0.01(2 - cot\alpha)^{2.1} \; for \; cot\alpha \leq 2 \\ 0.09 \quad for \; cot\alpha > 2 \end{cases}$$

$$b = \begin{cases} 1.5 + 0.42(2 - cot\alpha)^{1.5} \; with \; a \; max \; of \; 2.35 \; for \; cot\alpha \leq 2 \\ 1.5 \qquad\qquad\qquad\qquad for \; cot\alpha > 2 \end{cases}$$

The EurOtop (2018) formulae were mostly fitted to experimental measurements under unimodal wind sea conditions, with additional guidance to account for bimodal sea conditions. Coefficient values that are equivalent to cot α = 1.5 and cot α = 3.0 will be used for comparison against the experimental results in Equation (4).

3 Experimental Set-up

The Swansea University Coastal Laboratory facility includes an Armfield wave tank 30m in length, 1m metres in width and 1.2 m in depth. Waves are generated with an HR Wallingford computer-controlled piston paddle which has the capability to reproduce user-defined spectra of different types, includes a second-order wave correction due to Schäffer and Klopman (2000) and it is also equipped with an active wave absorption system to minimize wave reflection. To model a more realistic bathymetry for the experiment, the seabed was modified to a foreshore slope of 1:20 in front of the structure which was positioned toward the far end of the tank to accommodate a large number of wavelengths as shown in Fig 1. A constant crest width of 0.40 m was tested in all the experiments. Overtopping volumes were collected using a chute fitted directly on top of the structure placed at the rear end of the crest. The chute emptied the water into the overtopping collection tank. The overtopping volume was obtained by measuring the water level in the tank before and after each test.

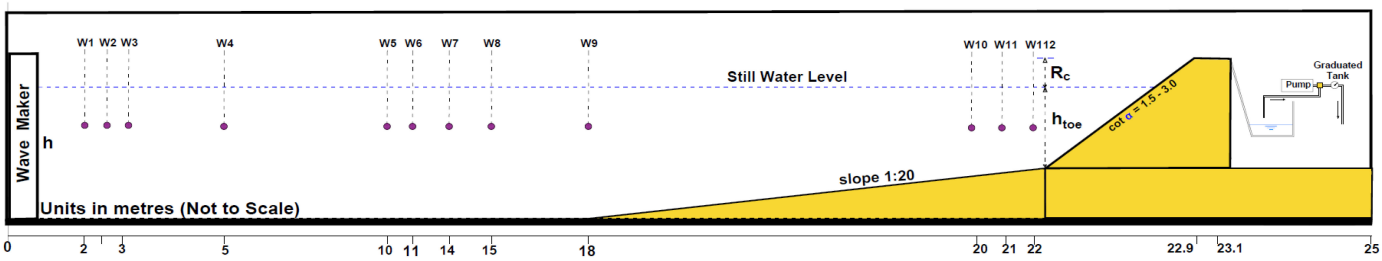

a

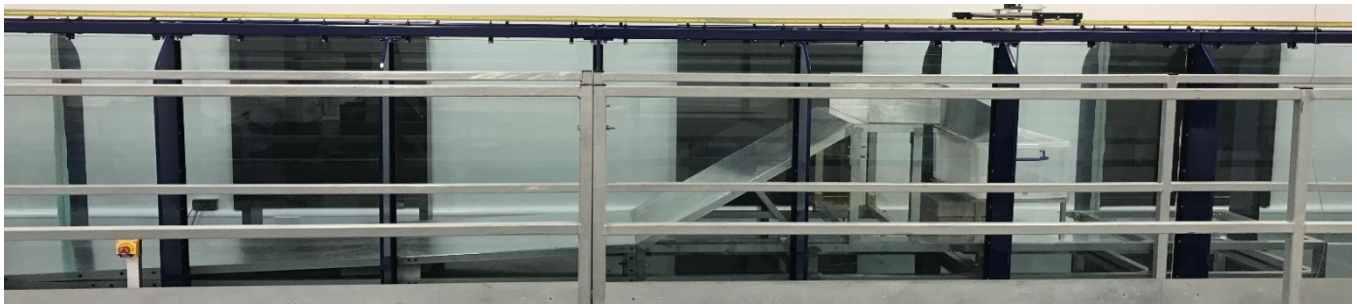

b

Fig 1. (a) Schematic cross section and (b) Photograph of the experimental set-up

3.1 Tested Wave Conditions

Fig. 2 shows an example of the energy-conserved bimodal spectrum used in this study. The spectrum contains different swell percentages with different swell periods of the same energy content. As described in the previous section, tested unimodal sea state possesses simple wind sea configuration with a unimodal spectrum described as red colour in Fig. 2. Bimodal spectrum of the same energy was then derived by introducing the swell component with different percentages at different frequencies as shown in Fig. 2(b). Table 1 contains the ranges of parameters tested in this study. To accommodate more swell conditions, only three swell percentages (25, 50 and 75 percentages) and four different swell peak periods of 1.739, 2.372, 3.162 and 3.953 seconds, which are equivalent to 11, 15, 20 and 25 seconds at prototype scales as shown in the figure, were tested. These were run across three crest freeboards as stated in Table 1. This implies that, including the wind sea state, 13 physical model tests were conducted for each case.

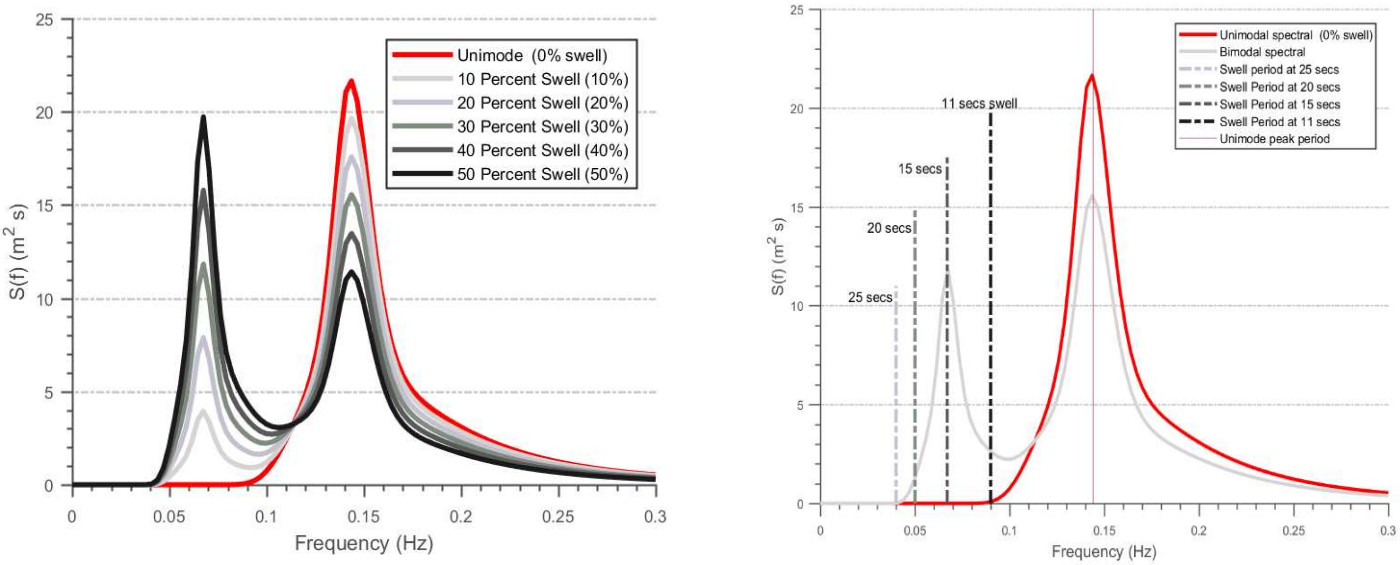

a b

Fig 2. An example of the tested energy-conserved bimodal spectrum showing different: (a) swell percentages and (b) swell periods (Orimoloye et al., 2019).

For each test, sequences of a minimum of 1000 random waves were generated to physically replicate a storm duration under laboratory conditions. Wave steepness ranging from 0.01 to 0.07 were tested in this study. The spectral characteristics of the bimodal spectrum were determined. These include the narrowness parameter, the wave spectrum energy, the spectral wave height and the spectral wave periods.

Tab. 1. Ranges of Parameters Tested

Parameter (Unit)	Range
Spectral wave height H_{m0} (m)	0.03 – 0.18
Crest freeboard R_c (m)	0.10 – 0.20
Water depth at wave maker h (m)	0.60 – 0.70
Water depth at toe h_t (m)	0.49 – 0.59
Spectral wind-wave peak period $T_{wm\text{-}1,0}$ (s)	1.106 – 1.581
Spectral swell-wave peak period $T_{sm\text{-}1,0}$ (s)	1.739 - 3.952
Swell percentage S_w (%)	0, 25, 50, 75
Relative Freeboard R_c/H_{m0} (-)	0.80 – 4.00
Relative wave height H_{m0}/h (-)	0.07 – 0.26
Wave steepness $S_{m\text{-}1,0}$ (-)	0.01 – 0.07
Breaker parameter $\xi_{m\text{-}1,0\ (-)}$	2.4 – 5.5
Slope angle α (°)	33.70 and 18.43
Cot α (-)	1.5 and 3.0
Total successful tests (-)	546

4 Results

Figure 3 shows an example of how well the wavemaker reproduced different targeted unimodal and bimodal spectrum for different percentages of swell in the same sea state. The solid line represents the measured spectra, while the dotted line represents the theoretical target spectra. The wave gauge is placed at the middle distance (15 m) away from the wavemaker for an irregular bimodal sea condition with a significant wave height of 0.125 m and peak period $T_{m-1,0}$ of 1.1 s and a swell (secondary) peak period of 2.37 s. For the displayed spectra, a deep-water depth of 0.60 metres was used which was designed to an equivalent water depth of 0.45 at the toe of the structure. A reasonable level of agreement was achieved from the wave generation, although with some variations. Overall, the spectral peaks and shapes were reproduced to an acceptable level. The agreement was better in the unimodal cases than for the bimodal cases. Differences in deviations can be attributed to the complexities of physically generating bimodal waves, which require accommodation of the extended paddle motion needed to create longer period waves.

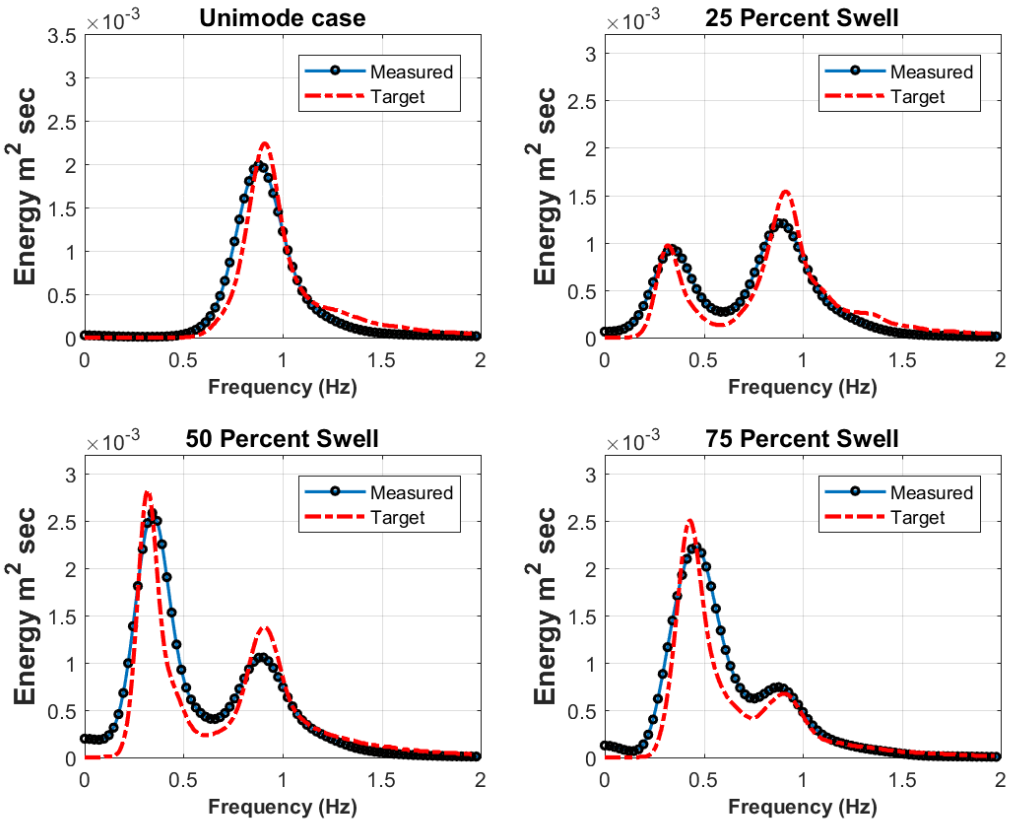

Fig 3. Comparison between the target bimodal spectrum for different percentages of swell with the same significant wave height.

The changes in the shapes of the spectra have been observed as essential parameters in wave bimodality. The dataset presented here contains the relationship between the dimensionless freeboard and the relative freeboard. The dataset is made up of 546 tests obtained from wave overtopping experiments conducted at the wave flume at the Swansea University Coastal Laboratory at the Department of Civil Engineering. The reflection analysis was performed using the HR-Daq data acquisition and processing software that was incorporated with the wavemaker control system. This package separates reflected waves from the total signals using the procedure from Zelt and Skjelbreia (1992). The spectra incident wave height (H_{m0}) at the toe of the structure were determined from the incident and reflected spectra from further analysis of observed wave overtopping datasets. As part of the study of each test, the dimensionless wave overtopping was determined.

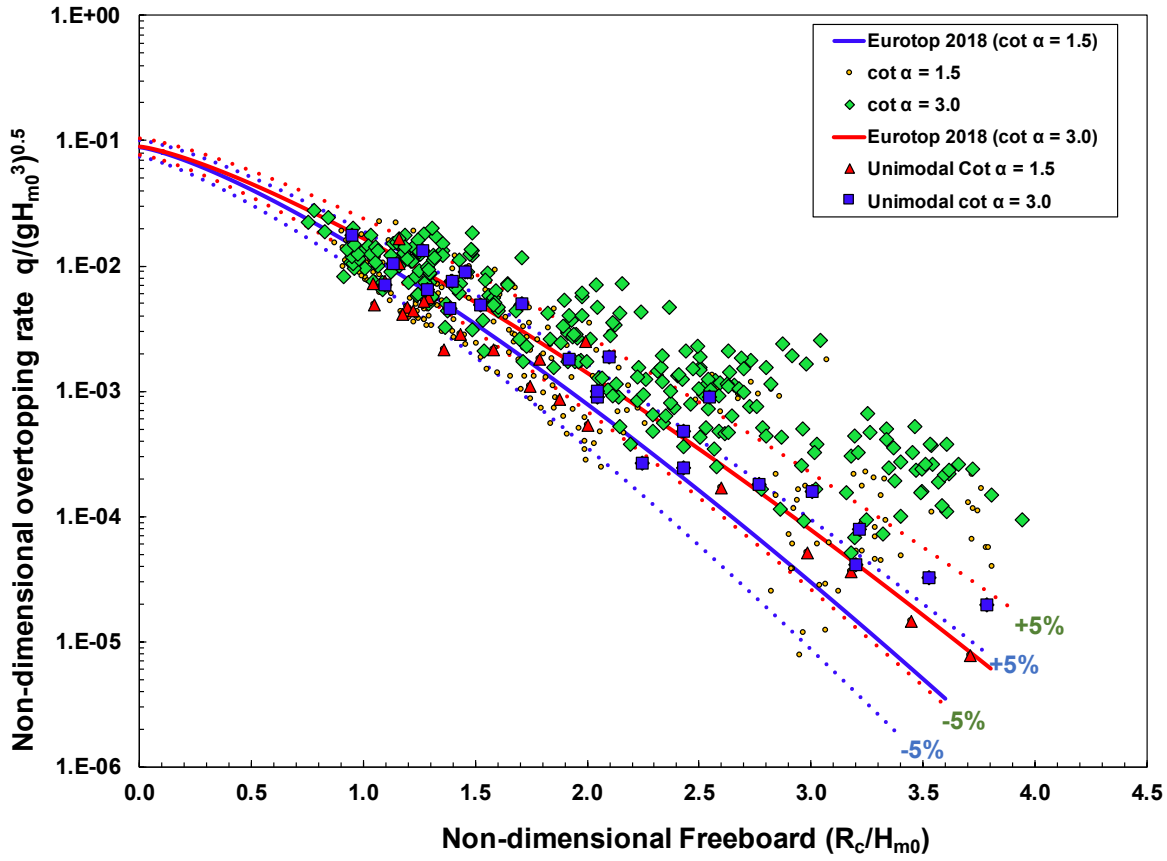

Fig 4. Non-dimensional overtopping rate $q/\sqrt{(H_{m03})}$ against non-dimensional crest freeboard R_c/H_{m0} for all tests captured for both unimodal and bimodal sea states across slopes with cot α = 1.5 and cot α = 3.0.

Fig. 4 shows non-dimensional average overtopping rate $q/\sqrt{(H_{m0}{}^3)}$ against non-dimensional crest freeboard R_c/H_{m0} for all 546 tests for both unimodal and bimodal sea states, for two seawall slopes (cot α = 1.5 and cot α = 3.0). It is evident from this figure that non-dimensional wave overtopping seems to be highly sensitive to the non-dimensional freeboard R_c/H_{m0} and the slope angle. As established in previous studies, non-dimensional wave overtopping $q/\sqrt{(H_{m0}{}^3)}$ reduces exponentially with the non -dimensional crest freeboard R_c/H_{m0} as presented by the semi-logarithm axis. As observed by Victor and Troch (2012), van der Meer and Bruce (2013), and Gallach-Sánchez et al. (2016), there is more scatter observed for larger values of relative freeboard compared to smaller ones. Moreover, the scatter patterns observed in these results follow the trend of slope angles previously reported in these studies. Specifically, Victor and Troch (2012) and Doorslaer et al. (2015) noted that non-dimensional wave overtopping slightly increases with increasing mildness of the slope. This is because less energy is reflected for milder slopes and gives room for more wave overtopping of the structure's crest. As also observed by Gallach-Sánchez et al. (2016), larger dimensionless crest freeboards R_c/H_{m0} are generally more sensitive to variations of slope angle than lower ones. The sensitivity of the datasets at larger dimensionless freeboards seems to be larger in the case of bimodal seas

Fig. 5 presents non-dimensional wave overtopping results of the steepest slopes studied with cot α = 1.5 (slope angle = 33.7°) for both unimodal and bimodal cases, together with the prediction and uncertainty intervals from the EurOtop (2018) non-breaking overtopping prediction formula that corresponds to this slope. The majority of the unimodal results fall within the 90 percent confidence intervals (-5% and +5%), whereas a significant number of bimodal cases lie outside these intervals, especially for larger freeboard, and are largely underpredicted by the EurOtop (2018) formula.

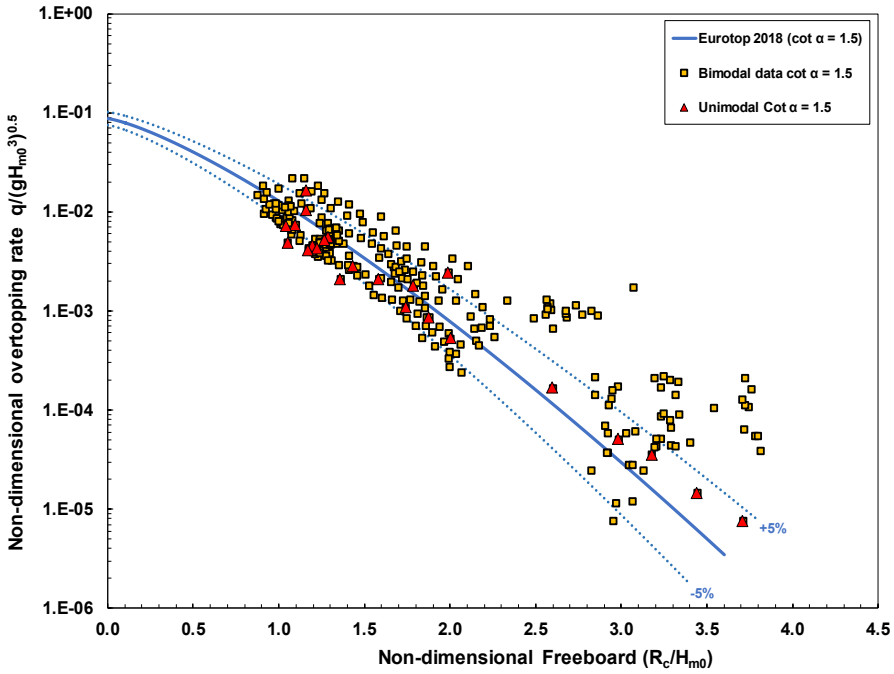

Fig 5. Non-dimensional overtopping rate $q/\sqrt{(H_{m0}{}^3)}$ against dimensionless crest freeboard R_c/H_{m0} for the dataset of cot α = 1.5 (unimodal and bimodal cases) compared to EurOtop (2018).

Non-dimensional wave overtopping under bimodal waves spreads beyond the confidence intervals and is more pronounced for values of $R_c/H_{m0} > 2.0$. It is hypothesized that this behaviour could be due to a greater shallow water effect in these conditions, although the implication seems to be diminished for milder slopes (cot α = 3.0) presented in Fig (6).

In the unimodal sea results presented, the influence of the mean wave period on the non-dimensional wave overtopping was not significant. The effects of wave period are more visible in spreading the scatter across the prediction ranges. This conclusion follows Victor and Troch (2012). However, wave periods have more significant effects in the case of the bimodal sea conditions.

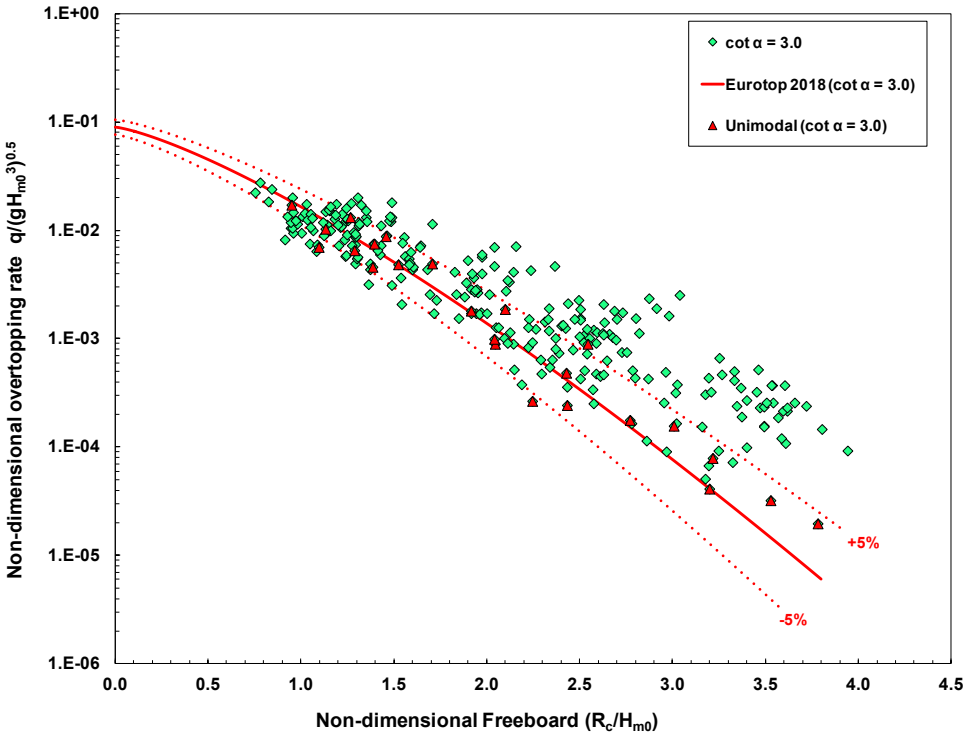

Fig 6. Non-dimensional overtopping rate $q/\sqrt{(H_{m0}{}^3)}$ against dimensionless crest freeboard R_c/H_{m0} for the dataset of cot α = 3.0 compared to EurOtop (2018).

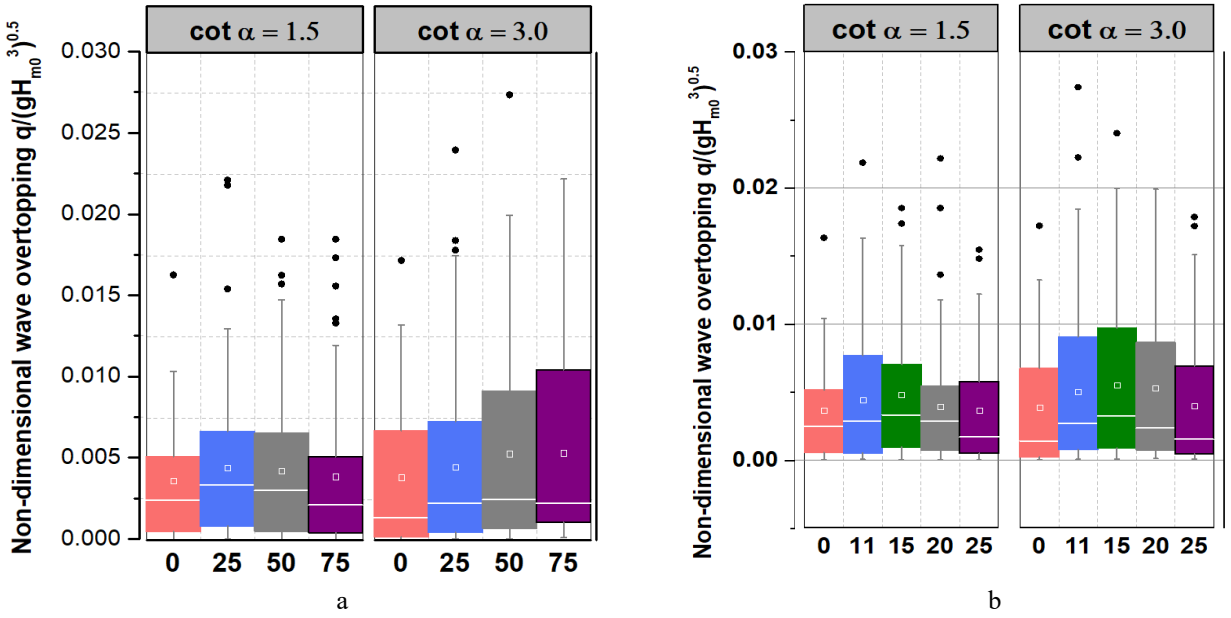

Fig 7. The relationship between the non-dimensional overtopping rate $q/\sqrt{(H_{m0}{}^3)}$ against the: (a) swell percentages and (b) Swell peak periods of cot α = 1.5 and cot α = 3.0.

Fig 7(a-b) shows how both swell percentages and swell periods are influencing the non-dimensional wave overtopping rate $q/\sqrt{(H_{m03})}$. These results are presented for two slopes (cot α = 1.5 and cot α = 3.0) investigated. As depicted in Fig 7(a), non-dimensional wave overtopping increases as swell percentages increases in the milder slope with cot α = 3.0 from the unimodal sea (swell percentage = 0) to the highest percentage of swell (swell percentage = 75). This behaviour slightly changes for the steeper slope (with cot α = 1.5). Swell percentages seem to increase only to 25 percent and then start to fall in value. The extreme values of non-dimensional wave overtopping are constant between both 50 and 75 percent swells, respectively. Fig 7(b) presents the case of the influence of swell peak periods on non-dimensional wave overtopping estimates. As visible in this part of the figure, more non-linear relationship exists between non-dimensional wave overtopping and changes in swell peak periods from 11 to 25 seconds. The non-dimensional wave overtopping seems to be highly sensitive to the swell peak periods. Swells occurring at higher frequencies (11 seconds in this case), tend to produce greater wave overtopping in both steeper and mild slopes as frequencies of swell reduces to 15, 20 and 25 seconds respectively. Non-dimensional wave overtopping seems to be highly sensitive to the difference between the spectral peak period of the wind sea and the swell spectral periods. Further research is still ongoing to better describe these relationships.

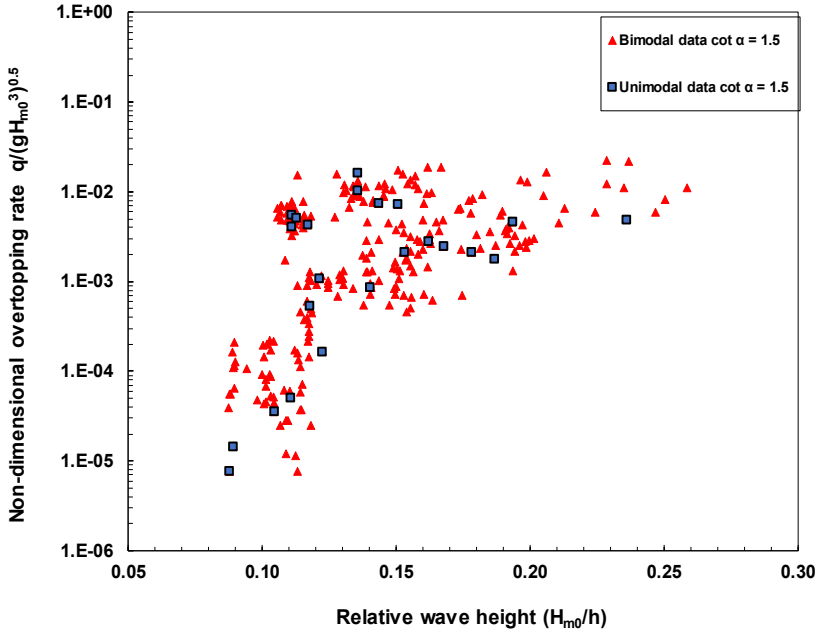

Fig 8. The relationship between the non-dimensional overtopping rate $q/\sqrt{(H_{m03})}$ against the relative wave height Hm0/h for the dataset of cot α = 1.5.

The influence of the relative wave height on the dimensionless wave overtopping across the two slopes for both unimodal and bimodal cases are each presented in Fig 8 (for cot α = 1.5) and Fig. 9 (for cot α = 3.0). The figures reveal that the majority of the observations fall within what may be categorized as deep-water conditions ($H_{m0}/h \leq 0.2$). The shallow water effects can be described in terms of this ratio. This ratio is also useful in describing the water depth condition within different test groups. As previously observed in Figs (4 - 6) that results for the steeper slope, (cot α = 1.5), show more scatter than for the milder slope, (cot α = 3.0), when the dimensionless freeboard is greater than 2.0. In deep-water conditions, no clear trend is observed in these results except for a small increase in the non-dimensional wave overtopping within the range $0.08 \leq H_{m0}/h \leq 0.12$ for the steepest slope (cot α = 1.5). Fig 8 shows that shallow water effects are less significant for the milder slope (cot α = 3.0). Nevertheless, there seems to be an increase in the minimum dimensionless wave overtopping with increasing relative wave height conditions.

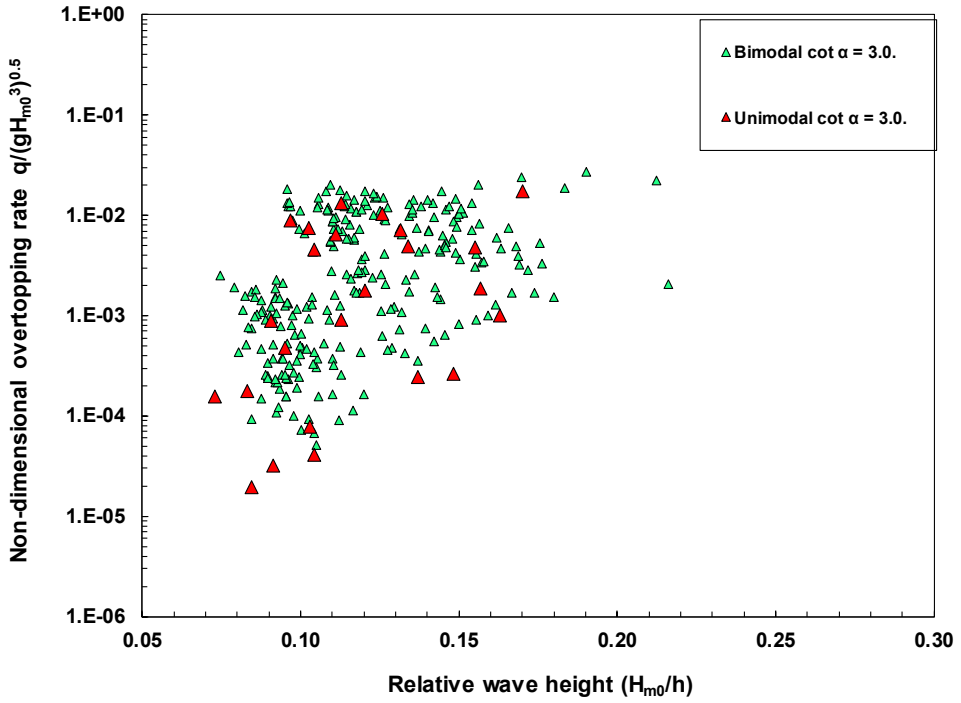

Fig 9. The relationship between the non-dimensional overtopping rate $q/\sqrt{(H_{m0}^3)}$ against the relative wave height H_{m0}/h for the dataset of cot α = 3.0.

5. Conclusions

The modelling of average wave overtopping performance of steep slopes under energy-conserved bimodal seas has been investigated using physical experiments conducted under laboratory conditions. A total of 546 overtopping tests were conducted at Swansea University Coastal Laboratory wave flume under deep water conditions with relative wave height H_{m0}/h ranging from 0.07 to 0.23. The non-dimensional wave overtopping results obtained for unimodal conditions are in good agreement with EurOtop predictions. Bimodal conditions show a more significant variability and are typically under-estimated by the EurOtop formula. Variation of non-dimensional wave overtopping with wall slope under bimodal conditions follows the trends found by other authors for unimodal conditions. Results for the bimodal case are sensitive to the difference between the spectral peak period of the wind sea to the swell spectral periods. The influence of swell spectral peak periods on non-dimensional wave overtopping is less clear and further research is required. We found that shallow water effects did not have a significant effect on wave overtopping in both unimodal and bimodal cases. Current research effortis focussed on investigating the influence of bimodal spectral characteristics on wave overtopping rates to provide refinements to the EurOtop (2018) formulae to more fully account for bimodal sea states.

References

Battjes, J. A. and Groenendijk, H. W. (2000) 'Wave height distributions on shallow foreshores', Coastal Engineering, 40(3), pp. 161–182. doi: https://doi.org/10.1016/S0378-3839(00)00007-7.

Bradbury, A.P., Mason, T.E. and Poate, T., 2007, November. Implications of the spectral shape of wave conditions for engineering design and coastal hazard assessment-evidence from the english channel. In 10th International Workshop on Wave Hindcasting and Forecasting and Coastal Hazard Symposium North Shore, Oahu, Hawaii, November (pp.11–16).

Biesel, S. F. (1951) 'Etude theorique d'un type d'appareil a la houle', La Houille Blanche, 2.

Brodtkorb, P. A. et al. (2000) 'WAFO – a Matlab toolbox for the analysis of random waves and loads', in Proc. 10th Int. Offshore and Polar Eng. Conf., ISOPE, Seattle, USA, pp. 343–350.

Burcharth, H. F. (1978) 'The effect of wave grouping on on-shore structures', Coastal Engineering, 2, pp. 189–199. doi: https://doi.org/10.1016/0378-3839(78)90019-4.

Coates, T. T. and Hawkes, P. J. (1998) 'Beach recharge design and bi-modal wave spectra', Coastal Engineering Proceedings, 1(26).

Doorslaer, K. Van et al. (2015) 'Crest modifications to reduce wave overtopping of non-breaking waves over a smooth dike slope', Coastal Engineering, 101, pp. 69–88.

Franco, L. et al. (1994) 'Wave overtopping on vertical and composite breakwaters', Proceedings from 24th International Conference on Coastal Engineering Kobe, ASCE, New York.

Franco, L. et al. (2009) 'Prototype measurements and small-scale model tests of wave overtopping at shallow rubble-mound breakwaters: The Ostia-Rome yacht harbour case', Coastal Engineering, 56(2), pp. 154–165.

Gallach-Sánchez, D. et al. (2011) 'Wave overtopping at smooth impermeable steep slopes with low crest freeboards', Journal of Waterway, Port, Coastal, and Ocean Engineering. American Society of Civil Engineers, 140(6), pp. 334–343.

Gallach-Sánchez, D. et al. (2016) 'Experimental study of overtopping behaviour of steep low-crested coastal structures', Journal of Waterway, Port, Coastal, and Ocean Engineering. American Society of Civil Engineers, 140(6), pp. 334–343.

Goda, Y. et al. (1975) 'Laboratory investigation on the overtopping rates of coastal structures', Ports and harbour research institute, 14, pp. 3–44.

Hawkes, P. J. et al. (1998) 'Impacts of bimodal season beaches', Hr Wallignford Report, p. 80. doi: http://eprints.hrwallingford.co.uk/711/1/SR507.pdf.

Krogstad, H. E. and Arntsen, Ø. A. (2000) 'Linear Wave Theory with special consideration of Random Waves and Statistics', Lecture Note Series, Part B, 23, pp. 1–42.

Van der Meer, J. et al. (2018) 'EurOtop 2018, Manual on wave overtopping of sea defences and related structures an overtopping manual largely based on European research, but for worldwide application'.

Van der Meer, J. and Bruce, T. (2014) 'New physical insights and design formulas on wave overtopping at sloping and vertical structures', Journal of Waterway, Port, Coastal, and Ocean Engineering. American Society of Civil Engineers, 140(6), p. 4014025.

Van der Meer, J. W. et al. (2005) 'Database on wave overtopping at coastal structures', CLASH WP2 database, Infram, Marknesse, NL.

Van der Meer, J. W. et al. (2009) 'The new wave overtopping database for coastal structures', Coastal Engineering, 56(2), pp. 108–120.

Orimoloye, S. et al. (2019) 'Effects of swell on wave height distribution of energy-conserved bimodal seas', Journal of Marine Science and Engineering. Multidisciplinary Digital Publishing Institute, 7(3), p. 79.

Owen, M. (1982) 'Overtopping of sea defences', in Proceedings from Conference Hydraulic Modelling of civil Engineering Structures BHRA University of Warwick, Coventry, pp. 469–480.

Pullen, T. et al. (2007) EurOtop 2007: Wave overtopping of sea defences and related structures: Assessment Manual. Available at: http://www.overtopping-manual.com.

Reeve, D. et al. (2015) Coastal Engineering: Processes, Theory and Design Practice. Spon Press.

De Rouck, J. et al. (2005) 'Report on field measurements petten sea defence: Storm Season 2003-2004', Coastal Engineering 2006: (In 5 Volumes). RIKZ, 5, pp. 29–43.

Rouck, J. De et al. (2009) 'Crest level assessment of coastal structures – General overview', Coastal Engineering, 56(2), pp. 99–107.

Rychlik, I. et al. (1997) 'Modelling and statistical analysis of ocean-wave data using transformed gaussian processes', Marine Structures, 10, pp. 13–47. doi: https://doi.org/10.1016/S0951-8339(96)00017-2.

Schäffer, H. A. and Klopman, G. (2000) 'Review of multidirectional active wave absorption methods', Journal of Waterway Port Coastal and Ocean Engineering, pp. 88–97.

Thompson, A. D. et al. (2017) 'Modelling extreme wave overtopping at Aberystwyth Promenade', Water, (9), p. 663.

Troch, P. et al. (2004) 'Full-scale wave-overtopping measurements on the Zeebrugge rubble mound breakwater', Coastal Engineering. Elsevier, 51(7), pp. 609–628.

Victor, L. and Troch, P. (2012) 'Wave overtopping at smooth impermeable steep slopes with low crest freeboards', Journal of Waterway, Port, Coastal, and Ocean Engineering. American Society of Civil Engineers, 138(5), pp. 372–385.

Van der Werf, I. and van Gent, M. (2018) 'Wave overtopping over coastal structures with oblique wind and swell waves', Journal of Marine Science and Engineering. Multidisciplinary Digital Publishing Institute, 6(4), p. 149.